

PPAR γ Activation Protects against Hydrogen Peroxide-Induced Oxidative Stress and Apoptosis in Human Liver Cells

Lingzhi Wu^{1,a#}, Fang Chen^{2,3,b#}, Kailong Zhong^{4,c}, Yunqi An^{5,d},
Yangge Lv^{1,e*}, and Xiaofeng Wu^{2,3,f*}

¹Department of Pharmacy, the Affiliated Hospital of Jiaying University (the First Hospital of Jiaying), Jiaying, Zhejiang 314000, China

²Department of Pharmacy, the First Affiliated Hospital of Xiamen University, Xiamen, Fujian 361000, China

³Xiamen Key Laboratory for Clinical Efficacy and Evidence-Based Research of Traditional Chinese Medicine, Xiamen University, Xiamen, Fujian 361015, China

⁴Department of Pharmacy, Zhongshan Hospital (Xiamen), Fudan University, Xiamen, Fujian 361015, China

⁵Pharmacology and Toxicology, Rutgers University, Piscataway, NJ 08854, USA

^ae-mail: wulingzhi1992@163.com ^be-mail: fangchen@xmu.edu.cn ^ce-mail: beyondzkl@126.com

^de-mail: yunqi.an@rutgers.edu ^ee-mail: 00187829@zjxu.edu.cn ^fe-mail: h2009xiaofeng@163.com

Received August 17, 2025

Revised December 30, 2025

Accepted December 30, 2025

Abstract—The deleterious role of oxidative stress in liver damage is a growing problem, and effective therapeutic interventions are highly warranted. This study evaluated whether peroxisome proliferator-activated receptor gamma (PPAR γ) activation protects against H₂O₂-induced oxidative stress and apoptosis in human L02 hepatocytes. Cells pretreated with rosiglitazone, a PPAR γ agonist, were incubated with H₂O₂, and cell viability was assessed using CCK8 and LDH release assays 24 h after the treatment. The content of apoptotic cells was determined using Hoechst 33258 staining, and the levels of apoptosis-related proteins were determined by immunoblotting. In addition, several oxidative stress indicators were measured. Possible involvement of the nuclear factor erythroid 2-related factor (Nrf2) pathway was investigated using the Nrf2 inhibitor ML385. Rosiglitazone (20 μ M) increased cell viability and improved nuclear morphology in H₂O₂-treated L02 cells, possibly by increasing the Bcl-2/Bax ratio and reducing caspase-3 activation. Rosiglitazone also decreased reactive oxygen species and malonaldehyde levels, as well as increased the activities of catalase, glutathione peroxidase, and superoxide dismutase. Rosiglitazone also promoted nuclear translocation of Nrf2 and increased the antioxidant levels in H₂O₂-treated L02 cells. Inhibition of the Nrf2 pathway by ML385 partially abolished the rosiglitazone-induced amelioration of oxidative stress and apoptosis. We conclude that activation of PPAR γ protects liver cells against oxidative stress and apoptosis through the Nrf2 pathway.

DOI: 10.1134/S0006297925602473

Keywords: rosiglitazone, L02 cells, hepatotoxicity, ML385, Nrf2

INTRODUCTION

Liver damage is common in chronic conditions such as viral infections, metabolic diseases, excessive

alcohol and drug consumption, and autoimmune diseases [1, 2]. Both experimental and clinical evidence indicate that oxidative damage, inflammation, dysregulation of signaling pathways, and dysfunction of the innate immune system play critical role in the progression of liver damage [3]. As the largest detoxification organ in the body, the liver metabolizes a wide

* To whom correspondence should be addressed.

These authors contributed equally to this study.

range of compounds, a process that generates reactive oxygen species (ROS) as byproducts [4]. Excessive ROS production disrupts redox balance, ultimately leading to oxidative stress. Oxidative stress promotes lipid peroxidation, DNA damage, irreversible protein modifications, and alterations in signaling pathways involved in the regulation of gene transcription, protein expression, and apoptosis, eventually resulting in hepatic damage [5, 6]. Because of its high metabolic activity, the liver is particularly susceptible to oxidative stress, which is closely associated with the emergence and progression of various liver diseases. Therefore, developing novel therapeutic strategies, in particular, those targeting oxidative stress-induced death of hepatocytes, might contribute significantly to the treatment of liver diseases.

High concentrations of ROS inhibit expressions of the anti-apoptotic Bcl-2 protein [7]. Excessive ROS disrupt mitochondrial function, reduce cellular energy supply, and promote the release of cytochrome *c*, resulting in the activation of caspase-3, a key enzyme of the apoptotic cell pathway [8]. Activated caspase-3 cleaves essential cytoplasmic proteins, leading to DNA fragmentation in the nucleus, characteristic changes in the nuclear morphology [9], and ultimately apoptosis.

Nuclear transcription factor peroxisome proliferator-activated receptor gamma (PPAR γ) plays a central role in the regulation of glucose and lipid metabolism. Its synthetic agonists thiazolidinediones (TZDs), such as rosiglitazone and pioglitazone, are a class of oral antihyperglycemic agents used in clinical practice [10]. Although TZDs possess some side effects that limit their use for glycemic control, PPAR γ activation has been shown to exert protective effects in a broad range of other diseases [11, 12]. For instance, rosiglitazone protects against traumatic brain injury in rats by attenuating neuronal apoptosis and autophagy [13]. Pioglitazone increases the expression of tight junction proteins, improves intestinal barrier function, and attenuates dextran sodium sulfate-induced colitis [14]. Although some studies have reported that TZDs, particularly troglitazone (first-in-class drug), induce hepatotoxicity by altering the levels of liver enzymes, the incidence for such toxicity with rosiglitazone is substantially lower than that observed with troglitazone [15]. Newer TZD compounds, such as rosiglitazone and pioglitazone, have been reported to exhibit milder and reversible hepatic toxicity profiles [15, 16]. The beneficial effects of rosiglitazone on liver injury have been reported more often than its adverse effects. For example, pretreatment with rosiglitazone inhibited extracellular signal-related kinase/mitogen-activated protein kinase (ERK/MAPK) signaling and activation of nuclear factor kappa B pathway, thereby effectively pre-

venting the progression of acute liver damage [17]. Rosiglitazone caused 80% higher cell survival in mice with acute liver injury by reducing liver necrosis and apoptosis through the modulation of endoplasmic reticulum stress pathways [18]. These findings suggest that contrary to concerns regarding hepatotoxicity, recently developed TZD, such as rosiglitazone, protect the hepatic functions. Further studies are required to clarify the underlying mechanisms in order to establish confidence in their potential therapeutic application against clinical hepatotoxicity.

Collectively, previous studies suggest that the beneficial effects of PPAR γ activation are largely attributable to its anti-inflammatory action across a range of pathological conditions. However, the role of PPAR γ activation in the liver, particularly at the cellular level, has not yet been clarified. In the present study, we investigated whether rosiglitazone-induced PPAR γ activation protects human L02 hepatocytes against hydrogen peroxide (H₂O₂)-induced oxidative stress and apoptosis and explored the underlying molecular mechanism. Our findings may suggest additional therapeutic options for the treatment of liver diseases.

MATERIALS AND METHODS

Materials. Dulbecco's modified Eagle's medium (DMEM) and L02 cells from Jiangsu Kaiji Biotechnology (Nanjing, China), fetal bovine serum (FBS) from Gibco Invitrogen (USA), trypsin from Dingguo Changsheng Biotechnology (Beijing, China), lactate dehydrogenase (LDH) assay kit (A020-2-2) from the Jiancheng Bioengineering Institute (Nanjing, China) were used. Cell counting kit-8 (CCK-8) (C0037), nucleoprotein extraction kit (P0027), Hoechst 33,258 solution (C1017), and assay kits for malonaldehyde (MDA) (S0131S), ROS (S0035S), glutathione peroxidase (GPx) (S0056), catalase (CAT) (S0051), superoxide dismutase (SOD) (S0101S), oxidized glutathione (GSSG) (S0053), and reduced glutathione (GSH) (S0053) were obtained from the Beyotime Institute of Biotechnology (Shanghai, China). Rabbit anti-Bax (sc-70408) and anti-Bcl-2 (sc-7382) antibodies from Santa Cruz Biotechnology (USA); rabbit antibodies against caspase-3 (9662), Kelch-like ECH-associated protein 1 (Keap1) (8047), Nrf2 (12721), quinone oxidoreductase 1 (NQO1) (3187S), and heme oxygenase-1 (HO-1) (43966) from Cell Signaling Technology (USA), rabbit anti- β -actin (AP0731), anti-histone H3(BS40053) antibodies, and secondary antibodies from Bioworld Technology (USA) were used. Rosiglitazone and ML385 were from Sigma (USA).

Cell culture. Cells were grown in DMEM supplemented with 10% FBS and 0.4% streptomycin/penicillin in 5% CO₂ at 37°C in a humidified atmosphere

and used in the experiments after six passages after reaching ~80% confluency.

CCK-8 assay. The cytotoxicity of different concentrations of H_2O_2 was determined using the CCK-8 assay. For this, L02 cells were seeded into 96-well plates (1×10^4 cells/well) and incubated for 24 h at 37°C in a humidified atmosphere containing 5% CO_2 . Next, the cells were washed twice with PBS and pretreated with various concentrations of H_2O_2 (0, 200, 400, 600, 800, and 1000 μM) for 24 h after two. CCK-8 solution (10 μL) was added to and the cells were incubated for 1 h. The absorbance at 450 nm was then measured to calculate the concentration of H_2O_2 that inhibited cell growth by 50% (IC50) [19].

Treatments. Hepatocyte injury model was established by L02 cell exposure to 600 μM H_2O_2 . To investigate the protective effects of rosiglitazone, H_2O_2 -treated L02 cells were divided into five groups and incubated for 24 h with the following compounds: control (vehicle + vehicle); drug control (20 μM rosiglitazone + vehicle); H_2O_2 (vehicle + 600 μM H_2O_2); low-dose rosiglitazone (10 μM rosiglitazone + 600 μM H_2O_2); and high-dose rosiglitazone (20 μM rosiglitazone + 600 μM H_2O_2). Cells in the low- and high-dose rosiglitazone groups were pretreated with rosiglitazone for 2 h prior to H_2O_2 exposure. After 24 h of incubation, the cells were assessed using the CCK-8 and LDH release assays, Hoechst 33258 staining, and Western blotting.

To investigate the protective mechanism of rosiglitazone against H_2O_2 -induced oxidative stress and apoptosis, cells were divided into five groups: (1) vehicle + vehicle; (2) vehicle + 600 μM H_2O_2 ; (3) 5 μM ML385 + 600 μM H_2O_2 ; (4) 20 μM rosiglitazone + 600 μM H_2O_2 ; and (5) 20 μM rosiglitazone + 5 μM ML385 + 600 μM H_2O_2 . Cells in the 5 μM ML385 + 600 μM H_2O_2 group were pretreated with ML385 for 2 h, followed by incubation with ML385 and H_2O_2 for 24 h. Cells in the 20 μM rosiglitazone + 5 μM ML385 + 600 μM H_2O_2 group were pretreated with rosiglitazone and ML385 simultaneously for 2 h and then co-incubated with H_2O_2 for 24 h.

LDH release assay. The extent of cell death in H_2O_2 -treated cells using the LDH release assay. Cells were seeded in 96-well plates (3×10^5 cells per well) and treated as indicated, after which the activity of LDH released from the cells to the culture medium was determined at 450 nm with a microplate reader. LDH activity reflected membrane damage and H_2O_2 -induced cytotoxicity. The same cell density per well was used for subsequent experiments conducted in 6-well plates.

Hoechst 33258 staining was used to investigate whether rosiglitazone protected L02 cells against H_2O_2 -induced apoptosis. Cells treated with rosiglitazone and H_2O_2 were washed three times with PBS,

incubated in 0.5 mL of fixation buffer at 37°C for 10 min, washed three times with PBS, and stained with Hoechst 33258 at room temperature in the dark for 5 min, and examined under a fluorescence microscope [20].

Intracellular ROS and MDA assessment. Intracellular ROS levels were determined with a ROS assay kit based on the fluorescence probe 2,7-dichlorodihydrofluorescein diacetate (DCFH-DA) that is oxidized by ROS to fluorescent dichlorofluorescein (DCF). Thus, DCF fluorescence signal was used to detect the ROS content in the cells. After treatment with H_2O_2 and rosiglitazone, cells were incubated with DCFH-DA (10 μM in PBS) at 37°C for 30 min. Cells were then washed three times with PBS, collected, and analyzed for their fluorescence intensity with a flow cytometer at the excitation wavelength of 488 nm and emission wavelength of 535 nm. MDA levels were measured using a commercial MDA assay kit according to the manufacturer's instructions (S0131S, Beyotime, China).

Assessment of oxidative stress indicators. The content of GSH and GSSG and the activities of CAT, SOD, and GPx were detected using the corresponding commercial kits according to the manufacturers' instructions.

Western blotting. Expression of Bcl-2 and Bax and activation of caspase-3 was evaluated using antibodies against caspase-3 (dilution, 1 : 1000), Bax (1 : 1000), Bcl-2 (1 : 1000), Keap1 (1 : 1000), Nrf2 (1 : 1000), HO-1 (1 : 1000), NQO1 (1 : 1000), β -actin (1 : 3000), and histone H3 (1 : 500). Cells were incubated with lysis buffer (180 μL of RIPA buffer containing phenylmethylsulfonyl fluoride at a 9 : 1 ratio) on ice for 30 min and the lysate was centrifuged at 4°C at 12,000g for 10 min to obtain protein-containing supernatant. Nuclear extract was prepared using a nucleoprotein extraction kit. Briefly, the cells were washed twice with PBS, collected by centrifugation at room temperature at 1000g for 5 min, and homogenized in an ice-cold hypotonic buffer for 10 min. The lysate was centrifuged at 4°C at 3000g for 5 min; the precipitate was washed with the hypotonic buffer and centrifuged at 4°C at 5000g for 5 min. Finally, 0.2 mL of lysis buffer was added to the precipitate, and the samples were incubated on ice for 20 min before centrifugation at 4°C at 15,000g for 5 min. The obtained supernatant containing nuclear proteins was stored at -40°C.

After determining protein concentration, proteins were separated electrophoretically and transferred to polyvinylidene fluoride membranes. Following blocking overnight with 5% fat-free milk, the membranes were probed with primary antibodies at 4°C and then incubated with an appropriate secondary antibody conjugated with horseradish peroxidase (dilution, 1 : 5000) at room temperature for 2 h.

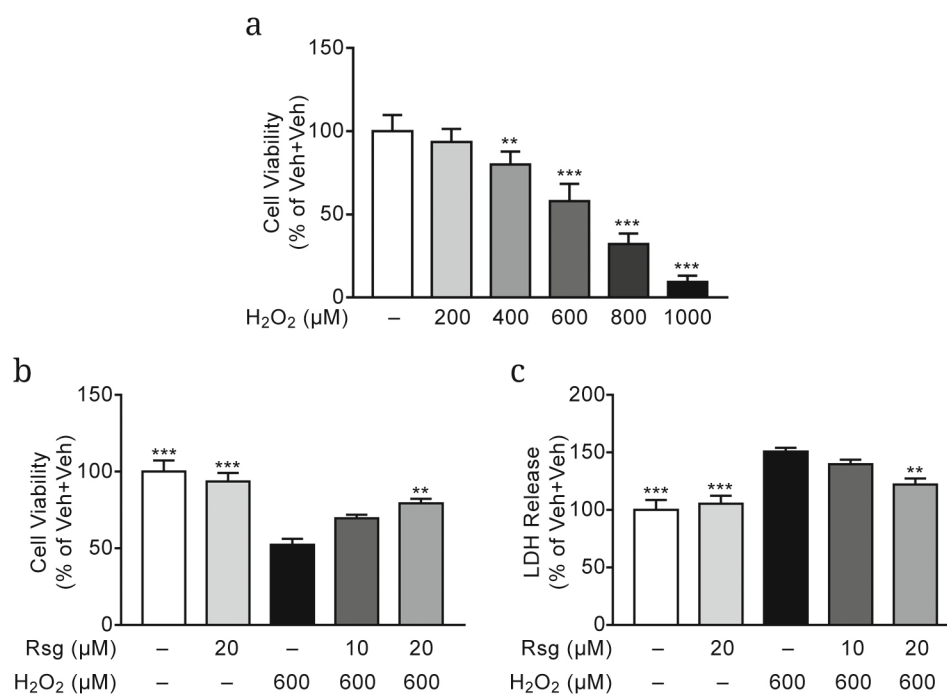


Fig. 1. PPAR γ activation ameliorates H₂O₂-induced cytotoxicity in L02 cells. a) Viability of L02 cells after 24-h exposure to different H₂O₂ concentrations (0, 200, 400, 600, 800, and 1000 μ M) as assessed by CCK-8 assay. b and c) Viability of L02 cells following indicated treatments assessed by CCK-8 (b) and LDH release (c) assays. Data are shown as mean \pm SEM ($n = 6$); ** $p < 0.01$, *** $p < 0.001$ vs. Veh + H₂O₂ group.

Protein bands were visualized using enhanced chemiluminescence with a gel imaging system (Tanon Science & Technology Co., China). Four biological repeats were performed for each Western blotting experiment.

Statistical analysis was performed with the SPSS software (version 20.0; IBM, USA). The results are expressed as mean \pm standard error of mean (SEM). Differences between the groups were evaluated using one-way ANOVA, followed by the Dunnett's *post hoc* test for multiple comparisons; p -value < 0.05 was considered statistically significant.

RESULTS

PPAR γ activation ameliorates H₂O₂-induced cytotoxicity in L02 cells. To determine the working concentrations of H₂O₂, L02 cells were exposed to different H₂O₂ concentrations for 24 h, followed by assessment of their viability using CCK-8 assay (Fig. 1a). Treatment with 600 μ M H₂O₂ reduced cell viability by ~50%; therefore, this concentration was selected for establishing the cell damage model. Next, we investigated whether rosiglitazone prevented H₂O₂-induced cytotoxicity in L02 cells using CCK-8 detection and LDH release assay. As shown in Fig. 1, the viability of H₂O₂-treated L02 cells was significantly decreased compared to the vehicle treatment group ($p < 0.001$,

Fig. 1b). Treatment with 10 μ M rosiglitazone slightly increased the viability of H₂O₂-treated cells, but the effect did not reach the level of statistical significance ($p > 0.05$, Fig. 1b). Rosiglitazone at the concentration of 20 μ M noticeably mitigated the H₂O₂-induced cytotoxicity, indicating a dose-dependent protective effect ($p < 0.01$, Fig. 1b). H₂O₂ exposure markedly increased the LDH release ($p < 0.001$), whereas pretreatment with 20 μ M rosiglitazone reduced it ($p < 0.01$, Fig. 1c). In vehicle-treated cells, rosiglitazone did not exert any cytotoxic effect ($p > 0.05$), as assessed by both CCK-8 and LDH release assays.

PPAR γ activation attenuates H₂O₂-induced apoptosis in L02 cell. Hoechst 33258 staining was used to evaluate the protective effect of rosiglitazone against H₂O₂-induced apoptosis in L02 cells. As shown in Fig. 2b, H₂O₂ treatment significantly increased the number of apoptotic cells compared to vehicle-treated controls ($p < 0.01$). L02 cells exposed to 600 μ M H₂O₂ for 24 h exhibited characteristic apoptotic features, including chromatin condensation and nuclear shrinkage, manifested as small, bright blue fluorescent dots (Fig. 2a). Pre-incubation with 20 μ M rosiglitazone exerted a protective effect on the cells ($p < 0.05$, Fig. 2b). Furthermore, treatment with rosiglitazone alone (20 μ M) did not induce apoptosis in vehicle-incubated cells. These results suggest that PPAR γ activation protects against H₂O₂-induced cell apoptosis.

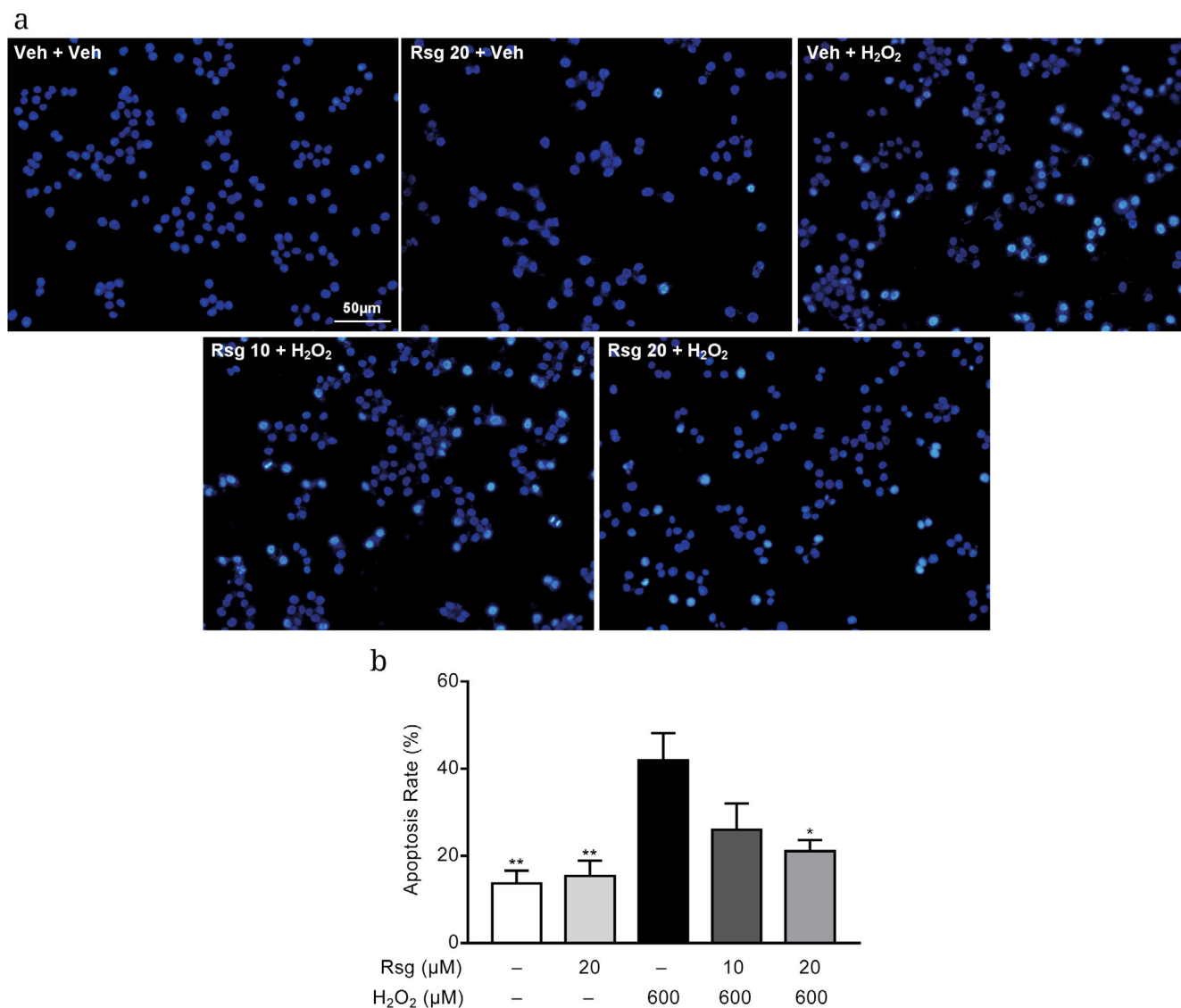


Fig. 2. PPAR γ activation inhibits H₂O₂-induced L02 cell apoptosis. a) Representative images of apoptotic L02 cells stained with Hoechst 33258. b) Cell apoptosis rate in treatments groups. Data are shown as mean \pm SEM ($n = 4$); * $p < 0.05$, ** $p < 0.01$, vs. Veh + H₂O₂ group.

PPAR γ activation increases the Bcl-2/Bax ratio and inhibits caspase-3 activation in H₂O₂-treated cells. To further investigate whether PPAR γ activation mitigates H₂O₂-mediated apoptosis, expression levels of Bax, Bcl-2, and caspase-3 were assessed by Western blotting. The results demonstrated that H₂O₂ significantly reduces the Bcl-2/Bax ratio ($p < 0.001$, Fig. 3, a and c) and elevated the level of caspase-3 ($p < 0.001$, Fig. 3, b and d) in L02 cells. Pretreatment with 20 μM rosiglitazone increased the of Bcl-2/Bax ratio ($p < 0.05$, Fig. 3, a and c). Rosiglitazone at 10 μM and 20 μM significantly inhibited caspase-3 activation ($p < 0.05$ and $p < 0.01$, respectively) (Fig. 3, b and d). Rosiglitazone (20 μM) treatment alone had no significant effect on the expression of these proteins in vehicle-incubated cells.

PPAR γ activation alleviates oxidative stress and enhances the antioxidative capacity in H₂O₂-treated cells. To evaluate the effect of PPAR γ activation on oxidative stress, we measured the content of ROS as key indicators of oxidative stress based on DCF fluorescence signal intensity. Treatment with H₂O₂ increased ROS levels ($p < 0.01$, Fig. 4a) in L02 cells compared to the vehicle group, while pretreatment with 20 μM rosiglitazone significantly reduced ROS accumulation in H₂O₂ treated-cells ($p < 0.05$, Fig. 4a). Similarly, the content of MDA (lipid peroxidation product) was elevated by oxidative stress ($p < 0.01$, Fig. 4b) in L02 cells, and pretreatment with 20 μM rosiglitazone markedly decreased its content in H₂O₂-incubated cells ($p < 0.05$, Fig. 4b). Moreover, H₂O₂ treatment decreased the activities

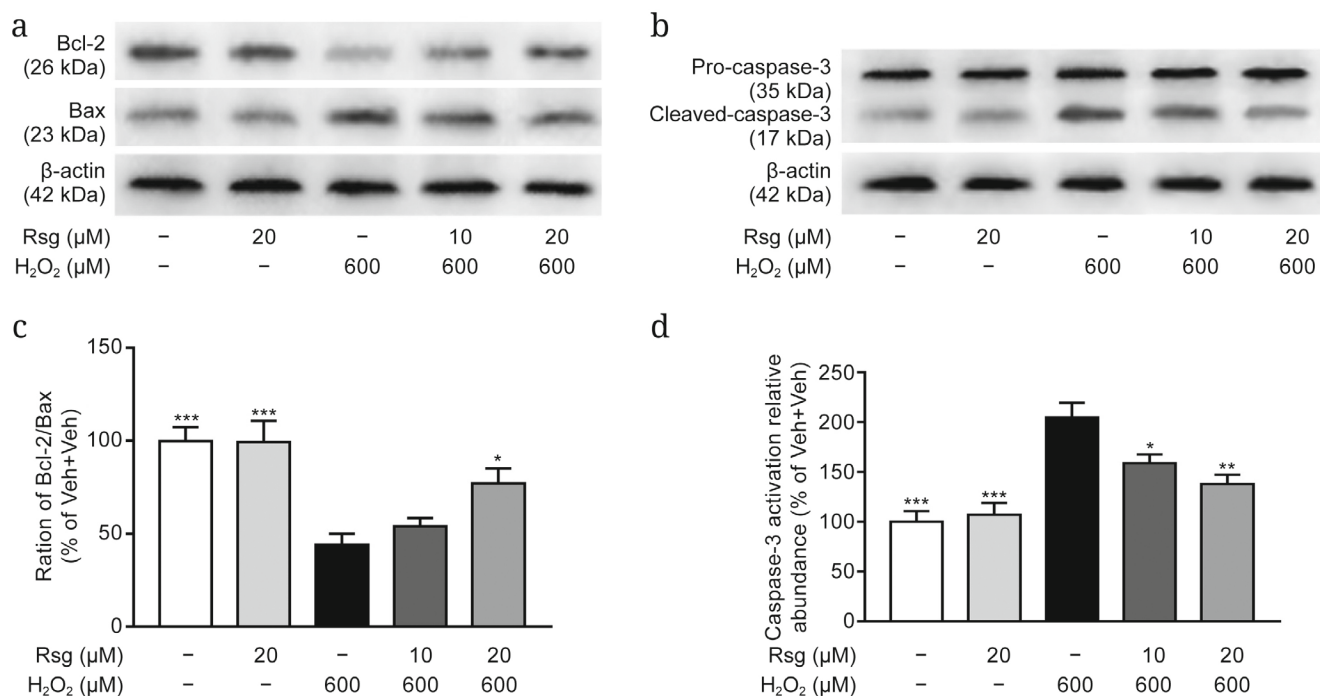


Fig. 3. PPAR γ activation increases Bcl-2/Bax ratio and inhibits caspase-3 activation in H₂O₂-treated cells. a and b) Protein expression levels of Bax, Bcl-2, procaspase-3, and cleaved caspase-3 as detected by Western blotting. c) Bcl-2/Bax ratio expressed as percentage of the Bcl-2/Bax in Veh + Veh group. d) Caspase-3 activation evaluated as the ratio of caspase-3 fragment to procaspase-3 and expressed as percentage of this ratio in Veh + Veh group. β -actin was used as an internal control. Data are shown as mean \pm SEM ($n = 4$); * $p < 0.05$, ** $p < 0.01$, *** $p < 0.001$ vs. Veh + H₂O₂ group.

of antioxidant enzymes, such as SOD ($p < 0.01$, Fig. 4c), CAT ($p < 0.05$, Fig. 4d), and GPx ($p < 0.01$, Fig. 4e), and increased the GSSG/GSH ratio ($p < 0.01$, Fig. 4f). Pretreatment with 20 μ M rosiglitazone restored the parameters to near-normal levels (SOD, $p < 0.05$, Fig. 4c; CAT, $p < 0.05$, Fig. 4d; GPx, $p < 0.05$, Fig. 4e; GSSG/GSH ratio, $p < 0.01$, Fig. 4f). At the same time, treatment with 20 μ M rosiglitazone alone had no significant effect on ROS levels, MDA content, antioxidant enzyme activities, or GSSG/GSH ratio in vehicle-treated cells.

PPAR γ activation stimulates Nrf2 signaling and expression of downstream antioxidant proteins in H₂O₂-treated cells. Western blot was performed to examine the Nrf2 pathway, which plays a crucial role in the regulation of cytoprotective responses against oxidative stress [21]. Under physiological conditions, Nrf2 binds Keap1, forming a complex that remains in the cytoplasm, thereby maintaining the pathway in an inactive state. Our data showed that H₂O₂ exposure increased the levels of cytoplasmic Nrf2 ($p < 0.01$, Fig. 5, a and c) and Keap1 ($p < 0.05$, Fig. 5, e and f), while markedly decreasing the content nuclear Nrf2 ($p < 0.05$, Fig. 5, b and d) compared to the vehicle group. Pretreatment with 20 μ M rosiglitazone significantly reduced cytoplasmic Nrf2 ($p < 0.05$, Fig. 5, a and c) and Keap1 ($p < 0.05$, Fig. 5, e and f) and concomitantly increased nuclear Nrf2 levels ($p < 0.05$, Fig. 5, b and d). Also, expression of the Nrf2 pathway

target proteins, such as HO-1 and NAD(P)H:quinone oxidoreductase 1 (NQO1), was assessed [22, 23]. Treatment with H₂O₂ decreased expression of both HO-1 ($p < 0.01$, Fig. 5, e and g) and NQO1 ($p < 0.01$, Fig. 5, e and h), but this effect was reversed by pretreatment with 20 μ M rosiglitazone ($p < 0.05$ for HO-1 and $p < 0.05$ for NQO1). Therefore, PPAR γ activation rescues the Nrf2 pathway suppressed by H₂O₂ and further upregulates expression of downstream target proteins.

PPAR γ -mediated protection against oxidative stress and cell apoptosis is partially abolished by Nrf2 inhibitor in H₂O₂-treated cells. To identify the signal transduction pathway through which PPAR γ activation protects against H₂O₂-induced oxidative stress and apoptosis, L02 cells were co-incubated with rosiglitazone and Nrf2 inhibitor ML385 (5 μ M) [24]. Coadministration of ML385 and rosiglitazone significantly attenuated the rosiglitazone-induced increase in cell viability ($p < 0.05$, Fig. 6a) and reversed rosiglitazone-mediated suppression of LDH release ($p < 0.05$, Fig. 6b) in H₂O₂-treated cells. Consistent with these observations, co-treatment with ML385 and rosiglitazone partially abolished rosiglitazone-mediated reduction of cell apoptosis ($p < 0.05$, Fig. 6, c and d).

PPAR γ -mediated protection against oxidative stress and cell apoptosis is partially abolished by Nrf2 inhibitor in H₂O₂-treated cells. Rosiglitazone-induced reduction in the levels of ROS ($p < 0.05$, Fig. 7a)

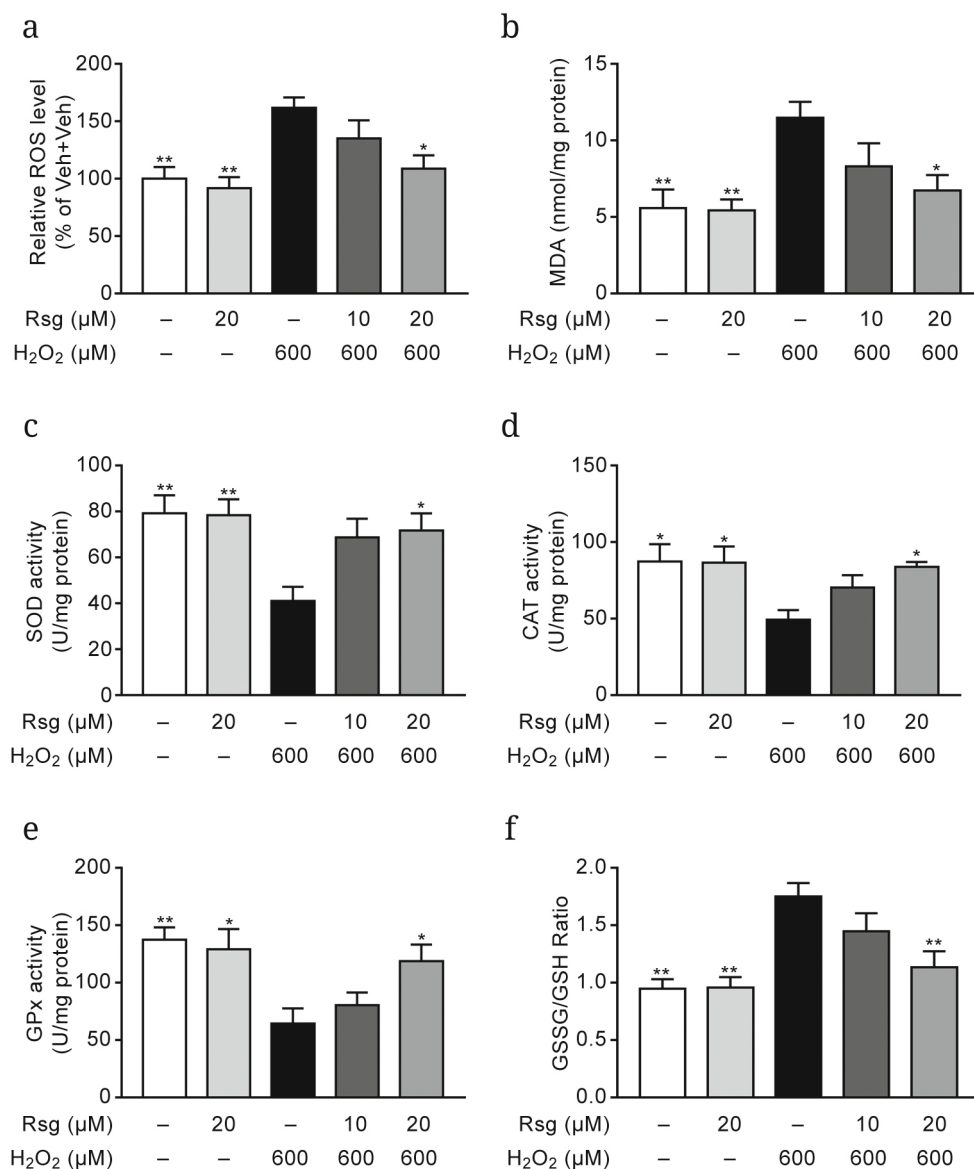


Fig. 4. PPAR γ activation alleviates oxidative stress and enhances antioxidant capacity in H₂O₂-treated cells. a) ROS levels in L02 cells expressed as percentage of DCF signal intensity relative to that in the Veh + Veh group. b) MDA levels. c-d) Activities of SOD (c), CAT (d), and GPx (e). f) GSSG/GSH ratio. Data are shown as mean \pm SEM ($n = 6$); * $p < 0.05$, ** $p < 0.01$, vs. Veh + H₂O₂ group.

and MDA ($p < 0.05$, Fig. 7b) was reversed by coadministration of ML385. Moreover, cotreatment with rosiglitazone and ML385 attenuated rosiglitazone-enhanced antioxidant defense in H₂O₂-treated cells, as indicated by the decreased activities of CAT ($p < 0.05$, Fig. 7d) and GPx ($p < 0.05$, Fig. 7e) and elevated GSSG/GSH ratio ($p < 0.05$, Fig. 7f). Although ML385 also reduced rosiglitazone-upregulated SOD activity in H₂O₂-treated cells, the effect was not statistically significant ($p > 0.05$, Fig. 7c).

Cytoprotective effect of PPAR γ activation against H₂O₂-induced injury is associated with the activation of Nrf2 pathway in L02 cells. Inhibition of Nrf2 attenuated rosiglitazone-mediated reduction

of cell apoptosis and improvement of antioxidant capacity, prompting us to use Western blotting to examine whether this protective effect was associated with the Nrf2 pathway. Coadministration of ML385 and rosiglitazone elevated cytoplasmic levels of Nrf2 ($p < 0.05$, Fig. 8, a and c) and Keap1 ($p < 0.05$, Fig. 8, e and f) downregulated by rosiglitazone, while rosiglitazone-enhanced nuclear Nrf2 level ($p < 0.05$, Fig. 8, b and d) was diminished. In line with the inhibition of Nrf2 nuclear translocation by ML385, coadministration of ML385 and rosiglitazone downregulated HO-1 expression level ($p < 0.05$, Fig. 8, e and g) in H₂O₂-treated cells compared to cells pretreated with rosiglitazone alone. Additionally, a trend toward

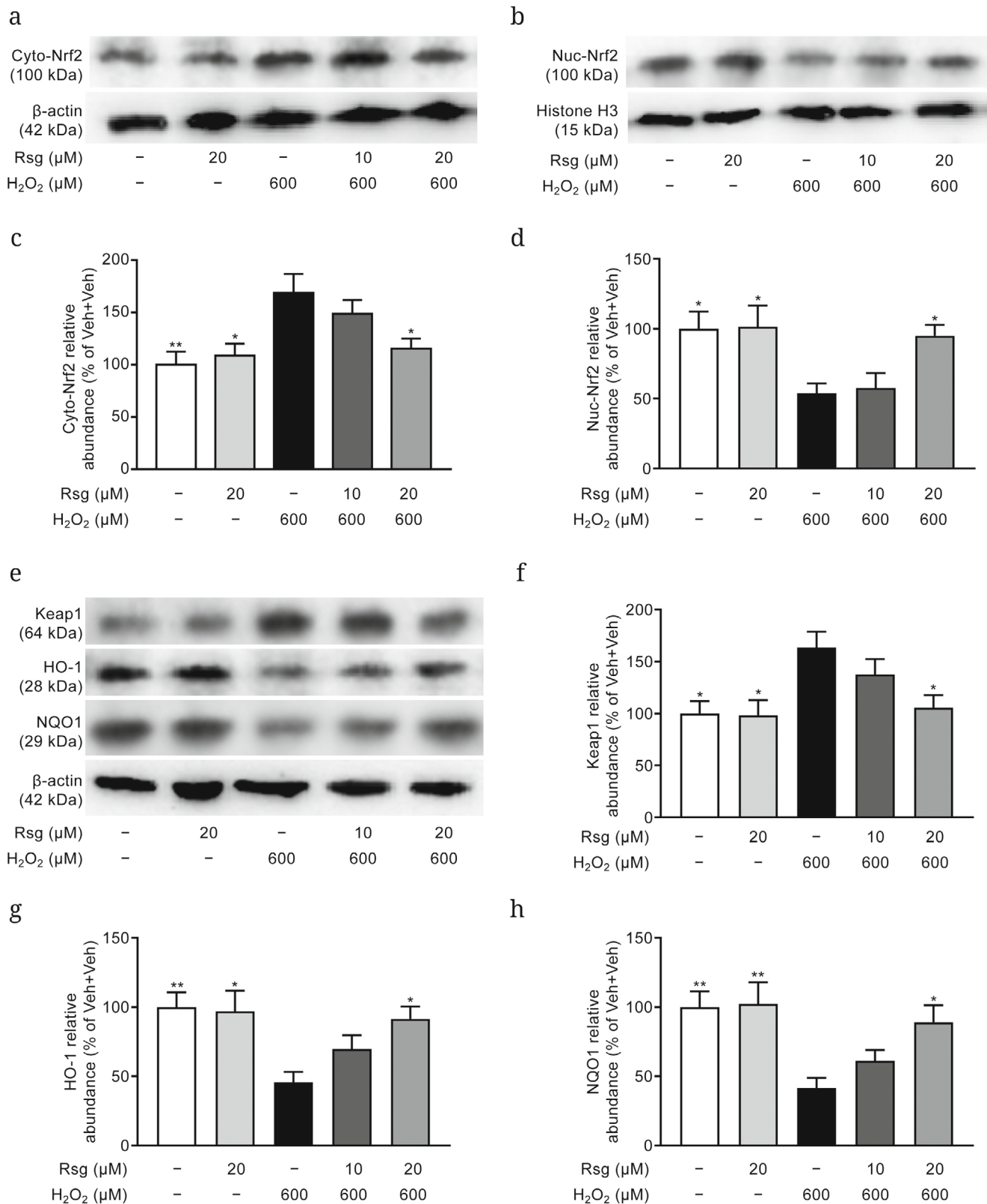


Fig. 5. PPAR γ activation stimulates Nrf2 signaling and expression of downstream antioxidant proteins in H₂O₂-treated cells. Protein levels of cytoplasmic Nrf2, nuclear Nrf2, Keap1, HO-1, and NQO1 were detected by Western blotting (a, b, and e). Quantification of cytoplasmic Nrf2 (c), nuclear Nrf2 (d), Keap1 (f), HO-1 (g), and NQO1 (h) is presented as a percentage of the corresponding values in the Veh + Veh group. β -Actin was used as an internal control for cytoplasmic and total protein, and histone H3 was used as an internal control for nuclear protein. Data are shown as mean \pm SEM ($n = 4$); * $p < 0.05$, ** $p < 0.01$, vs. Veh + H₂O₂ group.

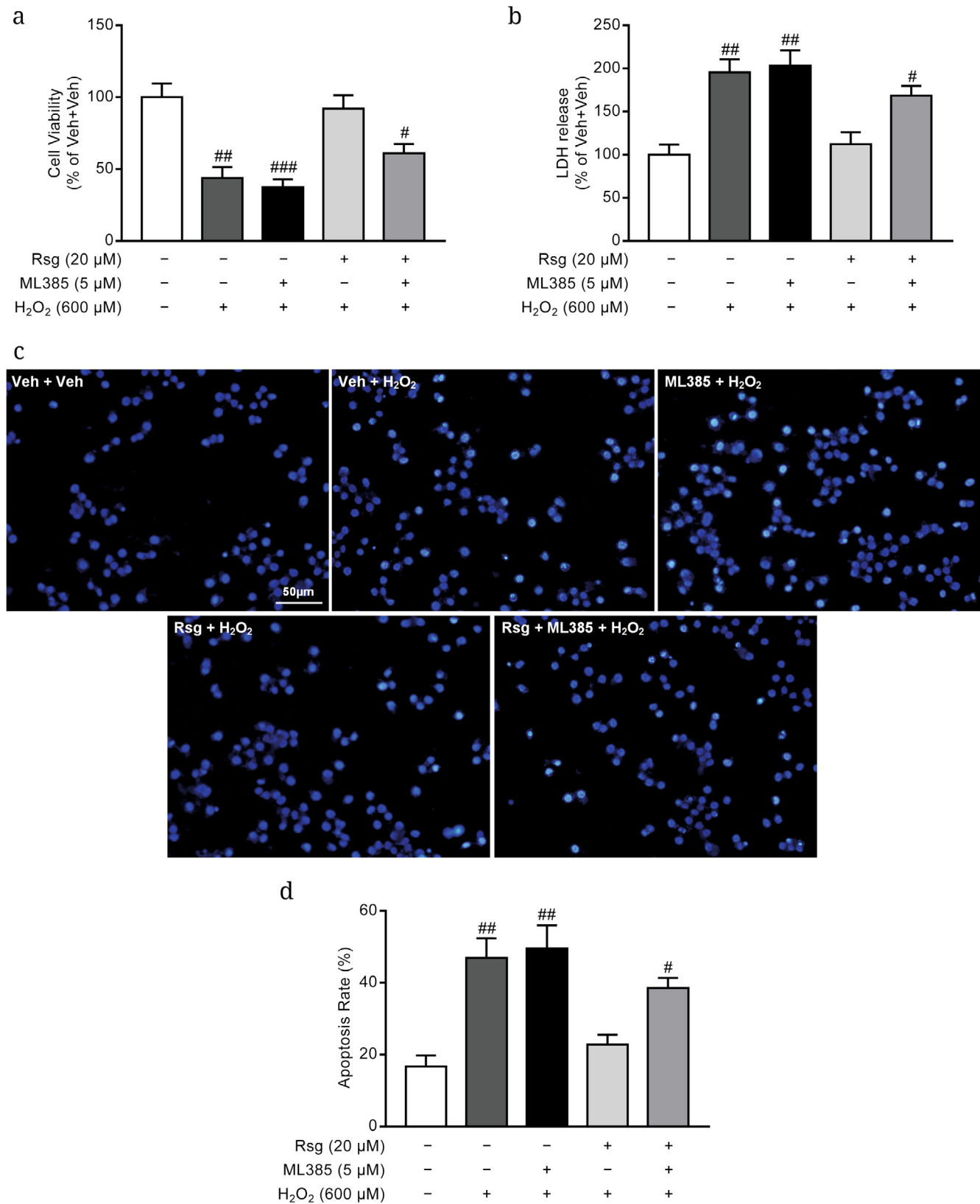


Fig. 6. Nrf2 inhibitor partially reverses the protective effect of PPAR γ activation against oxidative stress and cell apoptosis in H₂O₂-treated cells. Viability of L02 cells following indicated treatments assessed by CCK-8 (b) and LDH release (c) assays. c) Representative microphotographs of apoptotic cells stained by Hoechst 33258. d) Cell apoptosis rate in treatment groups. Data are shown as mean \pm SEM (for CCK-8 and LDH release assay, $n = 6$; for Hoechst 33258 staining, $n = 4$). # $p < 0.05$, ## $p < 0.01$, ### $p < 0.001$ vs. Rsg + H₂O₂ group.

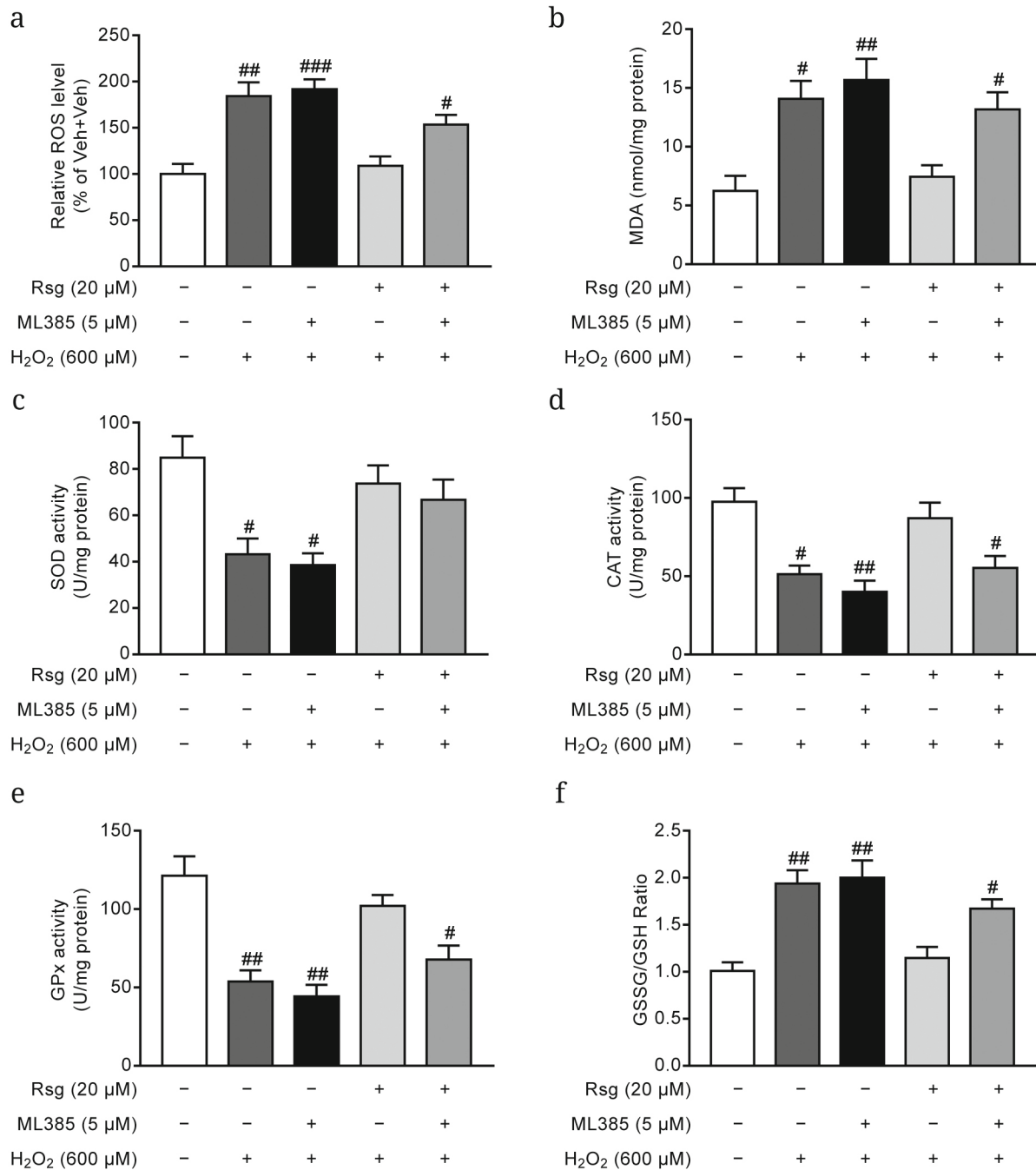


Fig. 7. PPAR γ -mediated protection against oxidative stress and cell apoptosis is partially abolished by Nrf2 inhibitor in H₂O₂-treated cells. a) ROS levels in L02 cells expressed as percentage of DCF signal intensity relative to that in the Veh + Veh group. b) MDA levels. c-d) Activities of SOD (c), CAT (d), and GPx (e). f) GSSG/GSH ratio. Data are shown as mean \pm SEM ($n = 6$); # $p < 0.05$, ## $p < 0.01$, ### $p < 0.001$ vs. Rsg + H₂O₂ group.

reduced NQO1 levels ($p > 0.05$, Fig. 8, e and h) was observed in H₂O₂-induced cells cotreated with ML385 and rosiglitazone, although this effect did not reach statistical significance relative to rosiglitazone administration alone. Collectively, these data indicate that the Nrf2 signaling pathway plays a critical role in the protective effect of PPAR γ activation against H₂O₂-induced oxidative stress and cell apoptosis.

DISCUSSION

The present study demonstrated that PPAR γ activation attenuates oxidative stress and apoptosis in L02 cells through the Nrf2 signaling pathways. Pretreatment with rosiglitazone at relatively higher concentration significantly enhanced cell viability and suppressed chromatin condensation in H₂O₂-treated

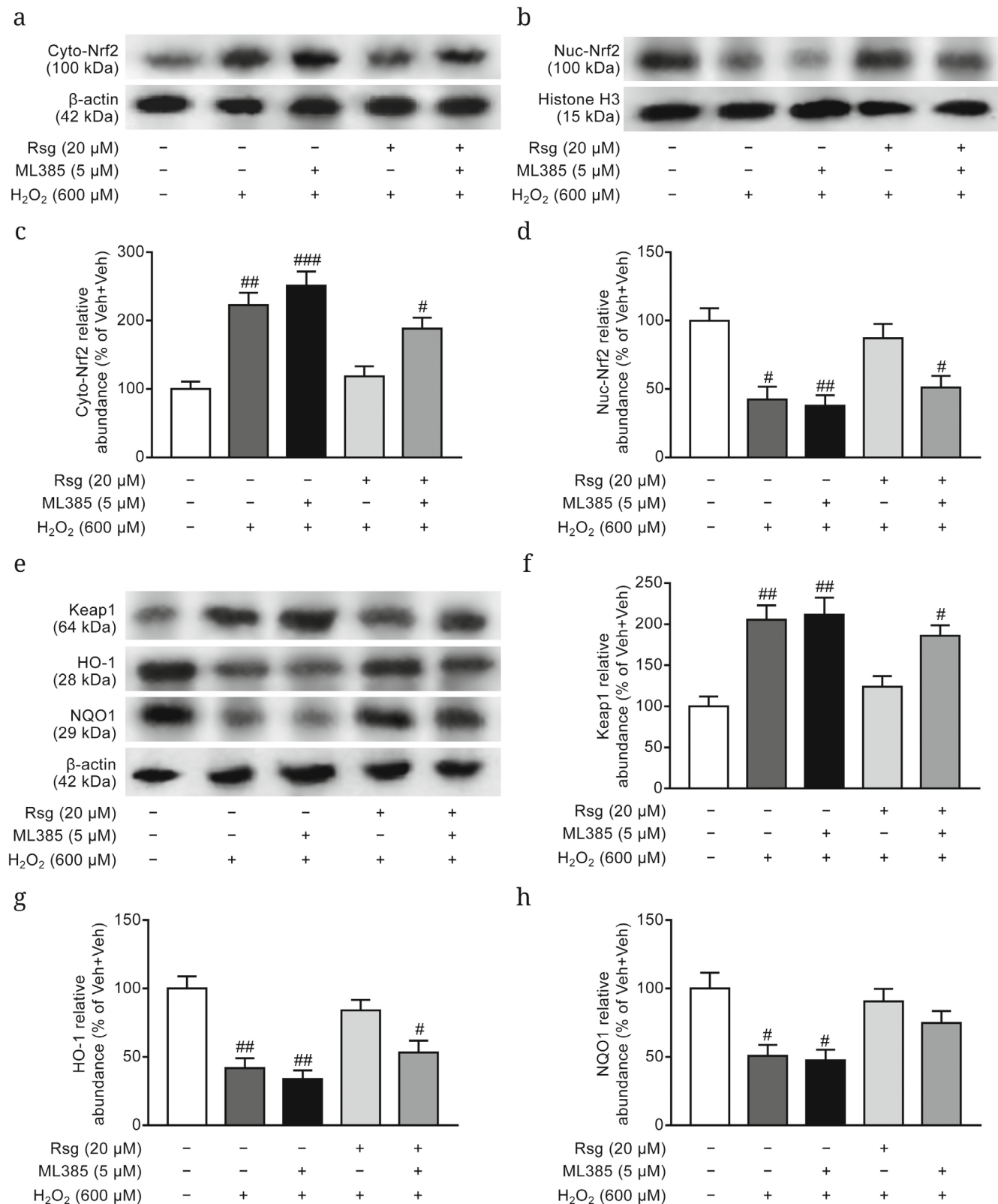


Fig. 8. Cytoprotective effect of PPAR γ activation against H₂O₂-induced injury in L02 cells is associated with the activation of Nrf2 pathway. a, b, and e) Protein levels of cytoplasmic Nrf2, nuclear Nrf2, Keap1, HO-1, and NQO1. Quantification of cytoplasmic Nrf2 (c), nuclear Nrf2 (d), Keap1 (f), HO-1 (g), and NQO1 (h) expressed as percentage of the corresponding values in the Veh + Veh group. β -Actin was used as an internal control for cytoplasmic and total protein, and histone H3 was used as an internal control for nuclear protein. Data are shown as mean \pm SEM ($n = 6$); # $p < 0.05$, ## $p < 0.01$, ### $p < 0.001$ vs. Rsg + H₂O₂ group.

L02 cells. Also, rosiglitazone pretreatment markedly reduced decreased ROS levels and MDA content, while restoring the activity of antioxidant enzymes, such as SOD, CAT, and GPx, indicating a significant mitigation of oxidative stress. Pretreatment with ML385 partially abolished the protective effects of rosiglitazone on cell viability and redox homeostasis in H₂O₂-exposed cells. Collectively, these findings suggest that PPAR γ activation protects against oxidative stress and cell apoptosis, an effect that is strongly associated with the Nrf2 pathway activation.

The onset and development of liver diseases may be explained by the development of oxidative stress, a key factor implicated in the pathogenesis of numerous hepatic disorders [25, 26]. ROS play an important role in several cellular functions, such as signal transduction, defense against harmful stimuli, and expression of genes involved in cell proliferation and death. However, excessive ROS accumulation that overwhelms endogenous antioxidant defense capacity disrupts redox homeostasis, leading to oxidative stress and severe cellular damage. H₂O₂ has a long lifetime and could easily convert to the highly reactive and cytotoxic hydroxyl radical [27]. H₂O₂ is widely used to induce the oxidative stress in various cell types [28, 29]. In the present study, exposure of L02 cells to 600 μ M H₂O₂ resulted in a reduced cell viability and oxidative stress induction, as evidenced by increased ROS levels, elevated MDA content, and suppression of the antioxidant defense system. Previous studies have reported that rosiglitazone inhibits inflammatory responses and reduces oxidative stress, thereby ameliorating renal tubular injury. Similarly, pioglitazone administration decreased the ROS levels while upregulating nitric oxide synthase phosphorylation and nitric oxide production, protecting aging cerebral arteries against oxidative stress damage [30]. Consistent with previous studies, our data demonstrate that administration of 20 μ M rosiglitazone reversed H₂O₂-induced oxidative damage in H₂O₂-treated L02 cells.

ROS are mainly generated in mitochondria; therefore, mitochondria are the primary organelles damaged by excessive ROS exposure. Mitochondrial DNA (mtDNA) is particularly susceptible to oxidative damage due to its unique structural features, lack of histone protection, and close proximity to the mitochondrial electron transport chain, a major site of ROS production [31]. Damage to mtDNA compromises ATP production and further enhances ROS generation. There is a growing body of evidence indicating that excessive mitochondrial ROS accumulation contributes to abnormal mitochondrial fission/fusion and calcium overload, which, in turn, promotes additional ROS production [32]. These pathological processes interact and form a vicious cycle that triggers apoptotic

signaling. Alterations in the Bax/Bcl-2 ratio promote the release of cytochrome *c* and trigger a caspase cascade, playing a critical role in mitochondrial dysfunction and oxidative stress-induced apoptosis. As a potent oxidant, H₂O₂ induces the permeability transition pore opening and increases mitochondrial permeability, leading to the caspase-dependent apoptosis in mammalian cells [33]. Here, we observed that H₂O₂-stimulated L02 cells exhibited chromatin condensation (a hallmark of apoptosis), reduced Bcl-2/Bax ratio, and elevated levels of cleaved caspase-3, a key executor of cell apoptosis. Previous studies [19] demonstrated that epigallocatechin-3-gallate alleviates high-fat diet-induced nonalcoholic fatty liver disease by inhibiting apoptosis through the ROS/mitogen-activated protein kinase pathway [19]. Similarly, melatonin attenuates oxidative stress, inhibits apoptosis in hepatocytes, and suppresses autophagy in animal models of acute liver failure [34]. In addition to the antioxidant effect, PPAR γ activation significantly reduced H₂O₂-induced cell apoptosis, supporting the idea that antioxidants exhibit protective effects and hold a strong therapeutic potential against hepatic injury.

The transcription factor Nrf2 is a cellular redox sensor expressed in multiple organs. Accumulating evidence indicates that chronic and severe stress can suppress Nrf2 activity and that dysregulation of the Nrf2 pathway is involved in the pathogenesis of several liver diseases [35]. We found that exposure to H₂O₂ elevated the Keap1 level and reduced nuclear translocation of Nrf2, thereby affecting the downstream antioxidant enzymes and reducing the antioxidant capacity of cells. The binding of ligands to PPAR γ activates it, leading to the PPAR γ translocation to the nucleus and interaction with the retinoid X receptor (RXR) partner protein. The formed complex binds to PPAR response elements (PPREs) located in the promoter regions of PPAR γ -regulated genes. Several studies have demonstrated that PPAR γ agonists enhance the PPAR γ transcriptional activity and upregulate the expression of key antioxidant proteins, such as HO-1, CAT, and GPx, thereby counteracting oxidative stress [36, 37]. Interestingly, a previous study identified several putative PPREs in the promoter region of *Nrf2* gene; however, their function significance remains unclear, suggesting a potential direct regulatory association between PPAR γ and Nrf2 [38]. This might partially explain how PPAR γ activation promotes Nrf2 translocation to the nucleus, elevates activities of SOD, CAT, and GPx, and upregulates HO-1 and NQO1 expression, enhancing the antioxidant defense. Consequently, rosiglitazone treatment increased cell viability and reduced apoptosis. ML385 inhibited activation of the Nrf2 pathway and attenuated rosiglitazone-induced upregulation of antioxidant enzyme activities and expressions.

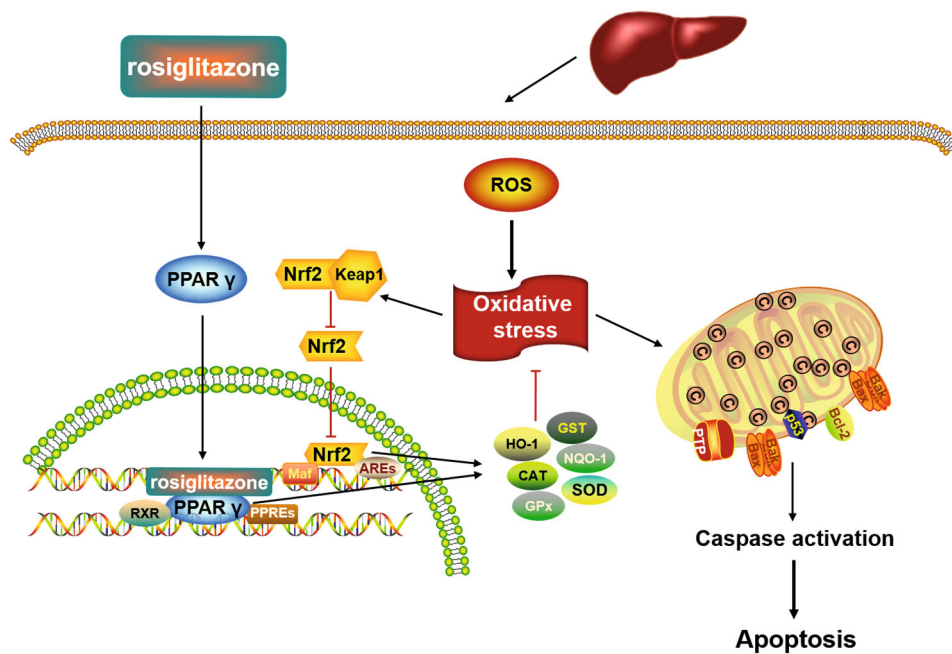


Fig. 9. Proposed mechanism by which rosiglitazone attenuates oxidative stress and apoptosis through activation of the Nrf2 signaling in L02 cells.

Coadministration of rosiglitazone and ML385 weakened the protective effect of rosiglitazone against oxidative stress and cell apoptosis. Intriguingly, several studies have identified antioxidant response elements (AREs) in the PPAR γ gene promoter region and demonstrated that increased nuclear translocation of Nrf2 upregulates PPAR γ expression [39, 40]. Nrf2 deletion significantly reduced PPAR γ expression *in vivo* [41]. We propose an existence of a crosstalk between the Nrf2 and PPAR γ pathways that creates a positive feedback loop and promotes expression of downstream antioxidant genes. Further studies are required to confirm the reciprocal regulation between PPAR γ and Nrf2 and to clarify the underlying signaling mechanisms.

CONCLUSION

PPAR γ activation protects cells against H₂O₂-induced oxidative stress through activation of the Nrf2 pathway, as indicated by increased activities of antioxidant enzymes (CAT, SOD, and GPx), upregulated expression of HO-1 and NQO1, and simultaneous increase in the Bcl-2 level, reduction in the Bax content, and caspase-3 activation (Fig. 9). Collectively, these findings suggest that PPAR γ activation holds significant therapeutic potential in prevention and/or treatment of liver disorders.

Abbreviations

CAT catalase
GPx glutathione peroxidase

HO-1 heme oxygenase-1
Keap1 Kelch-like ECH-associated protein 1
MDA malonaldehyde
Nrf2 nuclear factor erythroid 2-related factor 2
NQO1 NAD(P)H:quinone oxidoreductase 1
PPAR γ peroxisome proliferator-activated receptor gamma
PPRE PPAR response element
ROS reactive oxygen species
SOD superoxide dismutase

Contributions

L.Z.W., F.C., Y.G.L., and X.F.W. developed the study concept; L.Z.W., F.C., K.L.Z., and Y.Q.A analyzed the data; F.C., Y.G.L., and X.F.W. acquired the funding; L.Z.W. wrote the article draft; all authors reviewed and edited the manuscript.

Funding

This study was supported by Jiaxing Key Discipline of Medicine – Clinical Pharmacy (2023-ZC-008), Public Technology Application Research Program of Zhejiang Province of China (LGD21H310003), Science and Technology Project of Jiaxing of China (2021AD10023), Natural Science Foundation of Fujian Province (2024J011357), Natural Science Foundation of Xiamen (3502Z20227094), Project of Science and Technology of Xiamen City (3502Z20224ZD1024), and Xiamen Key Laboratory for Clinical Efficacy and Evidence-Based Research of Traditional Chinese Medicine.

Ethics approval and consent to participate

This work does not contain any studies involving human or animal subjects.

Conflict of interest

The authors of this work declare that they have no conflicts of interest.

Open access

This article is licensed under a Creative Commons Attribution 4.0 International License, which permits use, sharing, adaptation, distribution, and reproduction in any medium or format, as long as you give

appropriate credit to the original author(s) and the source, provide a link to the Creative Commons license, and indicate if changes were made. The images or other third party material in this article are included in the article's Creative Commons license, unless indicated otherwise in a credit line to the material. If material is not included in the article's Creative Commons license and your intended use is not permitted by statutory regulation or exceeds the permitted use, you will need to obtain permission directly from the copyright holder. To view a copy of this license, visit <http://creativecommons.org/licenses/by/4.0/>.

REFERENCES

1. Yan, Y., Jiang, W., Tan, Y., Zou, S., Zhang, H., Mao, F., Gong, A., Qian, H., and Xu, W. (2017) hucMSC exosome-derived GPX1 is required for the recovery of hepatic oxidant injury, *Mol. Ther.*, **25**, 465-479, <https://doi.org/10.1016/j.jymthe.2016.11.019>.
2. Basu, C., and Sur, R. (2018) S-allyl cysteine alleviates hydrogen peroxide induced oxidative injury and apoptosis through upregulation of Akt/Nrf-2/HO-1 signaling pathway in HepG2 cells, *Biomed. Res. Int.*, **2018**, 3169431, <https://doi.org/10.1155/2018/3169431>.
3. Heidari, R., Niknahad, H., Sadeghi, A., Mohammadi, H., Ghanbarinejad, V., Ommati, M. M., Hosseini, A., Azarpira, N., Khodaei, F., Farshad, O., Rashidi, E., Siavashpour, A., Najibi, A., Ahmadi, A., and Jamshidzadeh, A. (2018) Betaine treatment protects liver through regulating mitochondrial function and counteracting oxidative stress in acute and chronic animal models of hepatic injury, *Biomed. Pharmacother.*, **103**, 75-86, <https://doi.org/10.1016/j.biopha.2018.04.010>.
4. Cichoż-Lach, H., and Michalak, A. (2014) Oxidative stress as a crucial factor in liver diseases, *World J. Gastroenterol.*, **20**, 8082-8091, <https://doi.org/10.3748/wjg.v20.i25.8082>.
5. Seen, S. (2021) Chronic liver disease and oxidative stress – a narrative review, *Expert. Rev. Gastroenterol. Hepatol.*, **15**, 1021-1035, <https://doi.org/10.1080/17474124.2021.1949289>.
6. Chen, Z., Tian, R., She, Z., Cai, J., and Li, H. (2020) Role of oxidative stress in the pathogenesis of nonalcoholic fatty liver disease, *Free Radic Biol. Med.*, **152**, 116-141, <https://doi.org/10.1016/j.freeradbiomed.2020.02.025>.
7. Xu, P., Cai, X., Zhang, W., Li, Y., Qiu, P., Lu, D., and He, X. (2016) Flavonoids of *Rosa roxburghii* Tratt exhibit radioprotection and anti-apoptosis properties via the Bcl-2(Ca²⁺)/Caspase-3/PARP-1 pathway, *Apoptosis*, **21**, 1125-1143, <https://doi.org/10.1007/s10495-016-1270-1>.
8. Esteban-Fernández de Ávila, B., Ramírez-Herrera, D. E., Campuzano, S., Angsantikul, P., Zhang, L., and Wang, J. (2017) Nanomotor-enabled pH-responsive intracellular delivery of caspase-3: toward rapid cell apoptosis, *ACS Nano*, **11**, 5367-5374, <https://doi.org/10.1021/acsnano.7b01926>.
9. Alnahdi, A., John, A., and Raza, H. (2019) Augmentation of glucotoxicity, oxidative stress, apoptosis and mitochondrial dysfunction in HepG2 cells by palmitic acid, *Nutrients*, **11**, 1979, <https://doi.org/10.3390/nu11091979>.
10. Lebovitz, H. E. (2019) Thiazolidinediones: the forgotten diabetes medications, *Curr. Diab. Rep.*, **19**, 151, <https://doi.org/10.1007/s11892-019-1270-y>.
11. Yen, F. S., Wei, J. C., Chiu, L. T., Hsu, C. C., Hou, M. C., and Hwu, C. M. (2021) Thiazolidinediones were associated with higher risk of cardiovascular events in patients with type 2 diabetes and cirrhosis, *Liver Int.*, **41**, 110-122, <https://doi.org/10.1111/liv.14714>.
12. Wallach, J. D., Wang, K., Zhang, A. D., Cheng, D., Grossetta Nardini, H. K., Lin, H., Bracken, M. B., Desai, M., Krumholz, H. M., and Ross, J. S. (2020) Updating insights into rosiglitazone and cardiovascular risk through shared data: individual patient and summary level meta-analyses, *BMJ*, **368**, l7078, <https://doi.org/10.1136/bmj.l7078>.
13. Meng, Q., Chen, Z., Gao, Q., Hu, L., Li, Q., Li, S., Cui, L., Feng, Z., Zhang, X., Cui, S., and Zhang, H. (2022) Rosiglitazone ameliorates spinal cord injury via inhibiting mitophagy and inflammation of neural stem cells, *Oxid. Med. Cell Longev.*, **2022**, 5583512, <https://doi.org/10.1155/2022/5583512>.
14. Huang, Y., Wang, C., Tian, X., Mao, Y., Hou, B., Sun, Y., Gu, X., and Ma, Z. (2020) Pioglitazone attenuates experimental colitis-associated hyperalgesia through improving the intestinal barrier dysfunction, *Inflammation*, **43**, 568-578, <https://doi.org/10.1007/s10753-019-01138-3>.

15. Scheen, A. J. (2001) Hepatotoxicity with thiazolidinediones: is it a class effect? *Drug Safety*, **24**, 873-888, <https://doi.org/10.2165/00002018-200124120-00002>.
16. Isley, W. L. (2003) Hepatotoxicity of thiazolidinediones, *Expert Opin. Drug Safety*, **2**, 581-586, <https://doi.org/10.1517/14740338.2.6.581>.
17. Wang, J. X., Zhang, C., Fu, L., Zhang, D. G., Wang, B. W., Zhang, Z. H., Chen, Y. H., Lu, Y., Chen, X., and Xu, D. X. (2017) Protective effect of rosiglitazone against acetaminophen-induced acute liver injury is associated with down-regulation of hepatic NADPH oxidases, *Toxicol. Lett.*, **265**, 38-46, <https://doi.org/10.1016/j.toxlet.2016.11.012>.
18. Cao, Y., He, W., Li, X., Huang, J., and Wang, J. (2022) Rosiglitazone protects against acetaminophen-induced acute liver injury by inhibiting multiple endoplasmic reticulum stress pathways, *BioMed Res. Int.*, **2022**, 6098592, <https://doi.org/10.1155/2022/6098592>.
19. Wu, D., Liu, Z., Wang, Y., Zhang, Q., Li, J., Zhong, P., Xie, Z., Ji, A., and Li, Y. (2021) Epigallocatechin-3-gallate alleviates high-fat diet-induced nonalcoholic fatty liver disease via inhibition of apoptosis and promotion of autophagy through the ROS/MAPK signaling pathway, *Oxid. Med. Cell Longev.*, **2021**, 5599997, <https://doi.org/10.1155/2021/5599997>.
20. Shu, M., Lei, W., Su, S., Wen, Y., Luo, F., Zhao, L., Chen, L., Lu, C., Zhou, Z., and Li, Z. (2021) Chlamydia trachomatis Pgp3 protein regulates oxidative stress via activation of the Nrf2/NQO1 signal pathway, *Life Sci.*, **277**, 119502, <https://doi.org/10.1016/j.lfs.2021.119502>.
21. Zhang, H., Davies, K. J. A., and Forman, H. J. (2015) Oxidative stress response and Nrf2 signaling in aging, *Free Radic. Biol. Med.*, **88**, 314-336, <https://doi.org/10.1016/j.freeradbiomed.2015.05.036>.
22. Deng, S., Liu, S., Jin, P., Feng, S., Tian, M., Wei, P., Zhu, H., Tan, J., Zhao, F., and Gong, Y. (2021) Albumin reduces oxidative stress and neuronal apoptosis via the ERK/Nrf2/HO-1 pathway after intracerebral hemorrhage in rats, *Oxid. Med. Cell Longev.*, **2021**, 8891373, <https://doi.org/10.1155/2021/8891373>.
23. Mondal, N. K., Saha, H., Mukherjee, B., Tyagi, N., and Ray, M. R. (2018) Inflammation, oxidative stress, and higher expression levels of Nrf2 and NQO1 proteins in the airways of women chronically exposed to biomass fuel smoke, *Mol. Cell Biochem.*, **447**, 63-76, <https://doi.org/10.1007/s11010-018-3293-0>.
24. Ding, X., Jian, T., Li, J., Lv, H., Tong, B., Li, J., Meng, X., Ren, B., and Chen, J. (2020) Chicoric acid ameliorates nonalcoholic fatty liver disease via the AMPK/Nrf2/NFκB signaling pathway and restores gut microbiota in high-fat-diet-fed mice, *Oxid. Med. Cell Longev.*, **2020**, 9734560, <https://doi.org/10.1155/2020/9734560>.
25. Roghani, M., Kalantari, H., Khodayar, M. J., Khorsandi, L., Kalantar, M., Goudarzi, M., and Kalantar, H. (2020) Alleviation of liver dysfunction, oxidative stress and inflammation underlies the protective effect of ferulic acid in methotrexate-induced hepatotoxicity, *Drug Des. Dev. Ther.*, **14**, 1933-1941, <https://doi.org/10.2147/dddt.S237107>.
26. Yang, J., Fernández-Galilea, M., Martínez-Fernández, L., González-Muniesa, P., Pérez-Chávez, A., Martínez, J. A., and Moreno-Aliaga, M. J. (2019) Oxidative stress and Non-alcoholic fatty liver disease: effects of omega-3 fatty acid supplementation, *Nutrients*, **11**, 872, <https://doi.org/10.3390/nu11040872>.
27. Chen, Z., Wang, C., Yu, N., Si, L., Zhu, L., Zeng, A., Liu, Z., and Wang, X. (2019) INF2 regulates oxidative stress-induced apoptosis in epidermal HaCaT cells by modulating the HIF1 signaling pathway, *Biomed. Pharmacother.*, **111**, 151-161, <https://doi.org/10.1016/j.biopha.2018.12.046>.
28. Fu, J. Y., Jing, Y., Xiao, Y. P., Wang, X. H., Guo, Y. W., and Zhu, Y. J. (2021) Astaxanthin inhibiting oxidative stress damage of placental trophoblast cells *in vitro*, *Syst. Biol. Reprod. Med.*, **67**, 79-88, <https://doi.org/10.1080/19396368.2020.1824031>.
29. Tai, L., Huang, C. J., Choo, K. B., Cheong, S. K., and Kamarul, T. (2020) Oxidative stress down-regulates MiR-20b-5p, MiR-106a-5p and E2F1 expression to suppress the G1/S transition of the cell cycle in multipotent stromal cells, *Int. J. Med. Sci.*, **17**, 457-470, <https://doi.org/10.7150/ijms.38832>.
30. Wang, P., Li, B., Cai, G., Huang, M., Jiang, L., Pu, J., Li, L., Wu, Q., Zuo, L., Wang, Q., and Zhou, P. (2014) Activation of PPAR-γ by pioglitazone attenuates oxidative stress in aging rat cerebral arteries through upregulating UCP2, *J. Cardiovasc. Pharmacol.*, **64**, 497-506, <https://doi.org/10.1097/fjc.000000000000143>.
31. Wu, Z., Sainz, A. G., and Shadel, G. S. (2021) Mitochondrial DNA: cellular genotoxic stress sentinel, *Trends Biochem. Sci.*, **46**, 812-821, <https://doi.org/10.1016/j.tibs.2021.05.004>.
32. Nguyen, N. T., Nguyen, T. T., Da Ly, D., Xia, J. B., Qi, X. F., Lee, I. K., Cha, S. K., and Park, K. S. (2020) Oxidative stress by Ca²⁺ overload is critical for phosphate-induced vascular calcification, *Am. J. Physiol. Heart Circ. Physiol.*, **319**, H1302-H1312, <https://doi.org/10.1152/ajpheart.00305.2020>.
33. Li, D., Ni, S., Miao, K. S., and Zhuang, C. (2019) PI3K/Akt and caspase pathways mediate oxidative stress-induced chondrocyte apoptosis, *Cell Stress Chaperones*, **24**, 195-202, <https://doi.org/10.1007/s12192-018-0956-4>.
34. Song, J., Lu, C., Zhao, W., and Shao, X. (2019) Melatonin attenuates TNF-α-mediated hepatocytes damage via inhibiting mitochondrial stress and activating the Akt-Sirt3 signaling pathway, *J. Cell Physiol.*, **234**, 20969-20979, <https://doi.org/10.1002/jcp.28701>.

35. Ishida, K., Kaji, K., Sato, S., Ogawa, H., Takagi, H., Takaya, H., Kawaratani, H., Moriya, K., Namisaki, T., Akahane, T., and Yoshiji, H. (2021) Sulforaphane ameliorates ethanol plus carbon tetrachloride-induced liver fibrosis in mice through the Nrf2-mediated antioxidant response and acetaldehyde metabolism with inhibition of the LPS/TLR4 signaling pathway, *J. Nutr. Biochem.*, **89**, 108573, <https://doi.org/10.1016/j.jnuthbio.2020.108573>.
36. Cho, R. L., Yang, C. C., Tseng, H. C., Hsiao, L. D., Lin, C. C., and Yang, C. M. (2018) Haem oxygenase-1 up-regulation by rosiglitazone via ROS-dependent Nrf2-antioxidant response elements axis or PPAR γ attenuates LPS-mediated lung inflammation, *Br. J. Pharmacol.*, **175**, 3928-3946, <https://doi.org/10.1111/bph.14465>.
37. Chiang, M. C., Nicol, C. J., Cheng, Y. C., Lin, K. H., Yen, C. H., and Lin, C. H. (2016) Rosiglitazone activation of PPAR γ -dependent pathways is neuroprotective in human neural stem cells against amyloid-beta-induced mitochondrial dysfunction and oxidative stress, *Neurobiol. Aging*, **40**, 181-190, <https://doi.org/10.1016/j.neurobiolaging.2016.01.132>.
38. Kvandová, M., Majzúnová, M., and Dovinová, I. (2016) The role of PPAR γ in cardiovascular diseases, *Physiol. Res.*, **65**, S343-S363, <https://doi.org/10.33549/physiolres.933439>.
39. Xiong, L., Huang, J., Wang, S., Yuan, Q., Yang, D., Zheng, Z., Wu, Y., Wu, C., Gao, Y., Zou, L., and Hu, G. (2022) Yttrium chloride-induced cytotoxicity and DNA damage response via ROS generation and inhibition of Nrf2/PPAR γ pathways in H9c2 cardiomyocytes, *Arch. Toxicol.*, **96**, 767-781, <https://doi.org/10.1007/s00204-022-03225-1>.
40. Mahmoud, A. M., Hussein, O. E., Abd El-Twab, S. M., and Hozayen, W. G. (2019) Ferulic acid protects against methotrexate nephrotoxicity via activation of Nrf2/ARE/HO-1 signaling and PPAR γ , and suppression of NF- κ B/NLRP3 inflammasome axis, *Food Funct.*, **10**, 4593-4607, <https://doi.org/10.1039/c9fo00114j>.
41. Li, L., Fu, J., Liu, D., Sun, J., Hou, Y., Chen, C., Shao, J., Wang, L., Wang, X., Zhao, R., Wang, H., Andersen, M. E., Zhang, Q., Xu, Y., and Pi, J. (2020) Hepatocyte-specific Nrf2 deficiency mitigates high-fat diet-induced hepatic steatosis: involvement of reduced PPAR γ expression, *Redox Biol.*, **30**, 101412, <https://doi.org/10.1016/j.redox.2019.101412>.

Publisher's Note. Pleiades Publishing remains neutral with regard to jurisdictional claims in published maps and institutional affiliations. AI tools may have been used in the translation or editing of this article.